

A damped pendulum forced with a constant torque

P. Couillet,^{a)} J. M. Gilli, M. Monticelli, and N. Vandenberghe^{b)}
*Institut Non Linéaire de Nice, UMR 6618 CNRS - UNSA, 1361 Route des Lucioles, 06560,
Valbonne, France*

(Received 11 September 2003; accepted 19 August 2005)

The dynamics of a damped pendulum driven by a constant torque is studied experimentally and theoretically. We use this simple device to demonstrate some generic dynamical behavior including the loss of equilibrium or saddle node bifurcation with or without hysteresis and the homoclinic bifurcation. A qualitative analysis is developed to emphasize the role of two dimensionless parameters corresponding to damping and forcing. © 2005 American Association of Physics Teachers.
[DOI: 10.1119/1.2074027]

I. INTRODUCTION

Bifurcation theory allows a classification of the qualitative changes that occur in dynamical systems. A loss of equilibrium is the simplest bifurcation and occurs in many physical systems. A drop of water hanging at the end of a faucet is an example of such a bifurcation. We can make a small drop that hangs under the action of its weight, the action of the pressure of the surrounding fluid (water in the faucet and air), and the action of surface tension at the interface between water and air. The volume of the drop can be increased until a critical volume is reached. It is impossible to form a drop with a volume higher than this critical one.¹

In this paper, we focus on a mechanical example proposed by Andronov *et al.*² consisting of a damped pendulum forced by a constant torque. This system has been studied previously as a model of the pull-out torques of synchronous motors³ and as a model of a single point Josephson junction.⁴ It can be easily built and the physics involved in this device is very simple. The system has rich dynamical behavior and exhibits much more than a loss of equilibrium. Fundamental concepts such as hysteresis, bistability between equilibrium and periodic solutions, and homoclinic bifurcation will be explored.

The aim of the paper is to study the dynamics of the pendulum. Our main objective is to experimentally demonstrate bifurcations and complex dynamical behavior. We explore the two-dimensional parameter space and show that the different bifurcations separate three different regimes.

The paper is organized as follows. In Sec. II we introduce the experimental setup and the equation of motion. We show that the system is characterized by two dimensionless parameters. In Sec. III, we report the observed behavior with an emphasis on the bifurcations experienced by the pendulum. In Sec. IV we present a dynamical analog of the pendulum and an intuitive description of the dynamics. These three sections form a basic and intuitive introduction to qualitative dynamics, based on experiments and can be followed without any specific mathematical knowledge. In the more advanced Sec. V we use an analytical approach to present more quantitative results on the dynamics, in particular in the vicinity of the bifurcations. This section could form a basis for a problem accompanying an intermediate-level course on nonlinear dynamics.

II. EXPERIMENTAL SETUP AND EQUATION OF MOTION

A. Experimental setup

A planar pendulum is forced by a constant torque (see Fig. 1). The pendulum is linked to the drive shaft of a DC motor (with gearhead) through a magnetic coupler. This element is made of two coaxial disks (radius 4 cm) facing each other. One of the disks (M-disk) is attached to the drive shaft and has a few (8 in our case) neodym-iron-bore strong permanent magnets glued to its surface. The other disk (P-disk) is made of an aluminum alloy and is attached to the pendulum. The distance between the magnets and the P-disk can be changed between 0 and 1 cm. When the drive shaft rotates, eddy currents associated with an opposing Lorentz force⁵ are induced in the P-disk. The rotation of the motor induces a magnetic viscous torque on the pendulum, $T = \nu(\dot{\theta} - \Omega_m)$, where $\dot{\theta}$ is the angular velocity of the pendulum and Ω_m is the rotational speed of the motor. The viscous torque per unit of angular velocity, ν , depends on the strength of the magnets and the distance between the magnets and the P-disk. Moreover, the shaft of the pendulum is attached to the frame by ball bearings. The latter add a frictional torque which is more difficult to model. In the regime that we study, we assume that the frictional torque of the ball bearings is negligible compared to the torque caused by magnetic effects.

We use a voltage regulated power supply for the 7 W DC motor. The rotational speed of the motor is constant within 3% and can be easily modified by changing the applied voltage. The whole setup can be rotated about an axis perpendicular to the plane formed by the earth's gravitational field and the axis of rotation of the pendulum. Then the effective gravitational field is $g = g_0 \cos \alpha$, where $g_0 = 9.8 \text{ ms}^{-2}$ is the earth's gravitational field and α is the tilt angle between the rotation axis of the pendulum and the horizontal direction. During the experiment, we vary Ω_m and g .

We have deliberately chosen to describe qualitative experiments. We use a stopwatch to measure the period of oscillations of the pendulum and the rotational speed and a protractor to measure the angle of deviation at equilibrium. This measure gives the order of magnitude of different variables to help readers reproduce this experiment.

B. Equation of motion

The equation for the angular momentum of the pendulum is

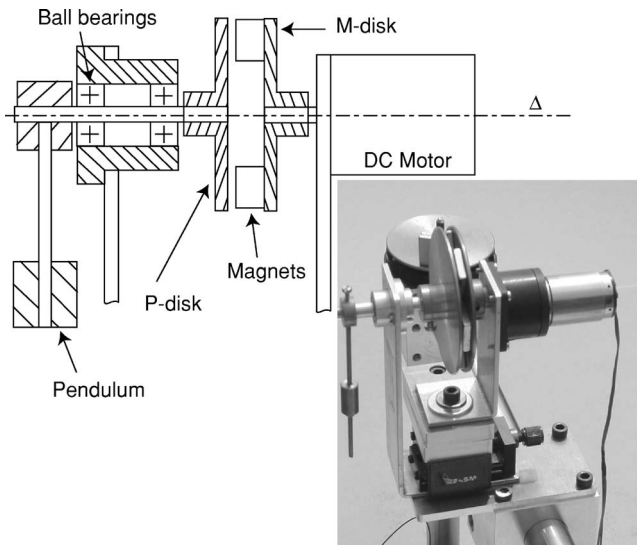


Fig. 1. Sketch and photograph of the experimental setup. The pendulum rotates about the axis Δ . The coupling between the pendulum and the motor is due to magnetic forces (there is no contact) between the aluminum disk (P-disk) attached to the pendulum and the disk with the magnets (M-disk) attached to the rotor of the motor.

$$I\ddot{\theta} + mg\ell \sin \theta = \nu(\Omega_m - \dot{\theta}) - \nu_a \dot{\theta}, \quad (1)$$

where I represents the moment of inertia of the pendulum, m is the mass of the pendulum, ℓ is the distance between the center of gravity of the pendulum and its axis of rotation, and ν is the viscous torque per unit of rotational speed due to the magnetic coupling. The parameter ν_a measures the frictional torque per unit angular velocity exerted on the pendulum by the surrounding air and the ball bearings. In this discussion ν_a will be neglected. The time is measured in units of the free oscillating period and the dimensionless time $\tau = (mg\ell/I)^{1/2}t$ will be used. The equation of motion reads

$$\theta' + \beta\theta' + \sin \theta = \gamma, \quad (2)$$

where \prime denotes the derivative with respect to τ , and

$$\beta = \frac{\nu}{\sqrt{mg\ell I}}, \quad \gamma = \frac{\nu\Omega_m}{mg\ell}. \quad (3)$$

The equilibria θ_e are solutions of

$$\sin \theta = \gamma. \quad (4)$$

III. EXPERIMENTS

A. Orders of magnitude

The parameter β can be measured using

$$\beta = \frac{\nu}{mg\ell} \sqrt{\frac{mg\ell}{I}} = \frac{a}{2\pi T_0}, \quad (5)$$

where a is the slope of $\sin \theta_e = f(\Omega_m)$, where Ω_m is measured in revolutions per second, and T_0 is the period of oscillations of the undamped pendulum (in its linear regime). The period is measured with a stopwatch and is approximately 1.0 s when $\alpha=0^\circ$ and 1.4 s when $\alpha=60^\circ$. From Fig. 2 we can determine the slope a for two series of measurements. The angular velocities are measured with a

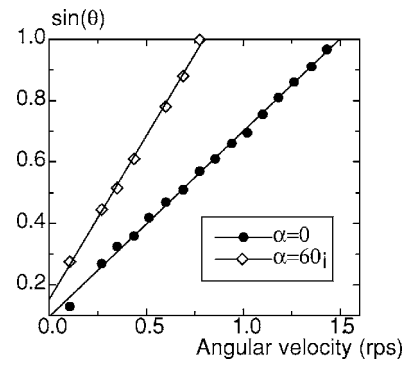


Fig. 2. Measurements of the sine of the angle of equilibrium vs the motor angular velocity for two different tilt angles of the pendulum.

stopwatch and the angle of tilt is measured with a protractor.

When the axis of the pendulum is horizontal, $\alpha=0$, we find $a_0=0.75$ (rps) $^{-1}$ and $\beta_0=0.8$. For $\alpha=60^\circ$, we find $a_{60}=1.5$ (rps) $^{-1}$ and $\beta_{60}=1.1$. We can verify that the ratio β_{60}/β_0 is approximately equal to $(\cos 0/\cos 60)^{1/2}=\sqrt{2}$ as given by Eq. (5) with $g=g_0 \cos \alpha$. Thus changing the angle α provides a way to change the effective value of the dissipation β . Another way would be to change the distance between the M-disk and the P-disk.

B. Dynamical experiments

Scenario 1: $\alpha=0$. When the motor does not rotate, the pendulum hangs at $\theta=0$. When the motor rotates slowly, the equilibrium state of the pendulum is tilted. When the rotational speed increases, the equilibrium approaches $\theta=\pi/2$, and at a critical velocity of the motor, Ω_c , the pendulum starts to rotate with a finite period of revolution. This transition to the rotating state corresponds to the loss of equilibrium.

If we return to a given velocity $\Omega_m < \Omega_c$ then the pendulum has a stable equilibrium at θ_s . We can perturb the pendulum, that is, we can release it without an initial velocity from an angle θ_i . If the perturbation is in the direction opposite to the motor rotation ($\theta_i < \theta_s$), the pendulum returns smoothly to its equilibrium. If we perturb the pendulum in the direction of the rotation, and if the angle of perturbation is small ($\theta_i < \pi - \theta_s$), the pendulum returns to equilibrium against the torque because gravity dominates. But if the initial angle is large enough ($\theta_i > \pi - \theta_s$), the pendulum does not go against the torque but moves in the direction of the torque.

If Ω_m is sufficiently large (but less than Ω_c), the pendulum starts to rotate and rapidly reaches a periodic regime. If we stop the pendulum by hand and put it close to its equilibrium state, it will stay in equilibrium. There is bistability between the rotating periodic regime and the stationary equilibrium. When we diminish Ω_m , the rotation of the pendulum slows, or in other words, the period of rotation increases. At a critical Ω_m , the pendulum stops. Before the pendulum stops, it tries to reach an angle higher than $\pi/2$ and then returns to its stable equilibrium. In this regime, if we perturb the pendulum, it returns to stable equilibrium, and there is no more rotating behavior.

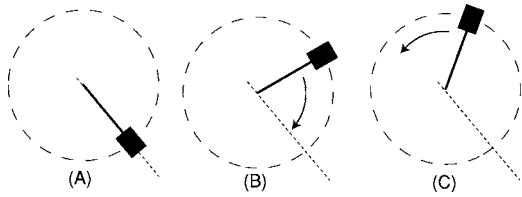


Fig. 3. Perturbation of the pendulum in for strong damping (scenario 2 in the text). The torque acts counterclockwise. (a) Stable equilibrium. (b) After a small perturbation, the pendulum returns directly to its stable equilibrium. (c) After a larger perturbation, the pendulum performs one revolution before returning to equilibrium.

If we increase Ω_m without perturbing the pendulum, the angle of equilibrium increases and reaches $\pi/2$ when $\Omega_m = \Omega_c$. For Ω_m slightly greater than Ω_c , the pendulum rotates quickly. There is a discontinuity in the behavior of the pendulum: It jumps to a periodic regime. If we decrease the speed of the motor, the pendulum continues rotating, even if the speed is less than Ω_c . The loss of equilibrium is a transition with hysteresis.

Scenario 2: $\alpha=60^\circ$. In this case the dimensionless dissipation β is higher. If the angular velocity is $\Omega_m < \Omega_c$, the equilibrium is tilted. If the pendulum is slightly perturbed by hand, it returns to equilibrium [Fig. 3(b)]. If the perturbation is strong enough, the pendulum carries out one rotation and then stops at stable equilibrium [Fig. 3(c)]. This behavior is called excitability: A perturbation higher than a given threshold is necessary to “fire” the system. But there is no periodic behavior in this regime when $\Omega_m < \Omega_c$. The equilibrium reaches the value $\pi/2$ for $\Omega_m = \Omega_c$ and for a higher angular velocity, there is no equilibrium. The pendulum rotates but the regime is very different from the one we found for a weaker dissipation: The period is very long and the pendulum spends a long time near $\theta = \pi/2$. In the rotating state, if Ω_m is decreased, as soon as $\Omega_m < \Omega_c$, the rotating state disappears and the pendulum stays at equilibrium.

IV. A POTENTIAL APPROACH

We now discuss the dynamics with a qualitative analog of the pendulum. The aim of this section is to give an intuitive understanding of the dynamics. We write the equation of motion in the form

$$\theta' + \beta\theta' = -\frac{\partial V(\theta)}{\partial \theta} \quad \text{with } V(\theta) = -\gamma\theta - \cos \theta. \quad (6)$$

We will describe the motion of a ball in the potential $V(\theta)$. The ball is acted on by its (normalized) weight and a viscous drag. The ball stays in contact with the potential. The motion of the ball is different from the motion of the pendulum because the kinetic energy has a different form.⁸ However, the qualitative behavior is the same, and, in particular, the equilibria are the same. We will discuss the motion of the pendulum and give a qualitative picture of the motion of the ball.

A. Periodic behavior and bistability

We start by considering the case of a nonforced conservative pendulum. The potential is simply $V(\theta) = -\cos \theta$. Stable equilibrium is at $\theta=0$ and unstable equilibrium is at $\theta=\pi$ [see Figs. 4(a) and 4(b)]. When we perturb the stable solu-

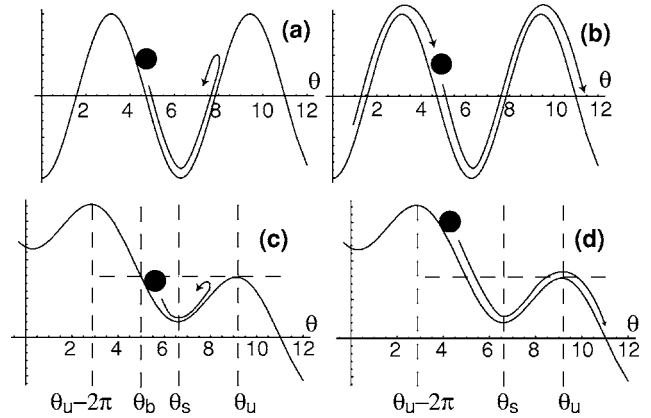


Fig. 4. Motion of a ball in a potential $V(\theta)$ without dissipation. Without forcing ($\gamma=0$), the ball (a) oscillates about the stable equilibrium or (b) moves indefinitely “from well to well.” With a weak forcing ($\gamma=0.3$) the ball (c) oscillates about the stable equilibrium or (d) falls indefinitely.

tion, the pendulum oscillates about its stable equilibrium. If we perturb it strongly, it will oscillate about the nearest stable equilibrium solution. With a sufficiently strong initial impulse, the pendulum will rotate indefinitely. There is a separatrix between those two types of behavior: The trajectory joining two successive unstable points, which is called a homoclinic trajectory. This trajectory is a limit case: If we release the pendulum from the unstable point or infinitely close to the unstable point, it takes an infinite time to escape from the vicinity of this point. Then it falls in the potential well and goes up again in an infinitely long time to the next unstable equilibrium.

When the external torque is slightly increased without dissipation (this case is not realistic in the experiment) [see Figs. 4(c) and 4(d)], the two equilibria move but still exist. We call θ_s the stable equilibrium and θ_u the unstable one. We call θ_b the value of θ at which the potential V has exactly the value $V(\theta_u)$. If we slightly perturb the system in stable equilibrium and start the pendulum with an angle between θ_b and θ_u and with no initial velocity, the pendulum oscillates about the stable solution. If the pendulum is released with an angle smaller than θ_b [see Fig. 4(d)], it will overshoot the next potential maximum and will accelerate forever. The first integral of Eq. (6) gives the speed increase between two successive unstable equilibria $\theta_2^2 - \theta_1^2 = 2(V(\theta_2) - V(\theta_1)) = 4\pi\gamma$. There is still a homoclinic trajectory serving as a separatrix between the oscillations and the rotations: It is the trajectory of the pendulum released from an angle infinitely close to but smaller than θ_u .

With weak dissipation, oscillations about θ_s are slightly damped. If we release the pendulum at θ_b , the ball will not reach θ_u . But if the dissipation is not too large, there is a point close to θ_b , call it θ_ℓ , such that if we release the pendulum at θ_ℓ , it will go asymptotically to θ_u . The point θ_ℓ must be consistent with an energetic balance between the energy dissipated because of damping and the change in potential energy. We multiply Eq. (6) by θ' and integrate between $\tau=0$ and $\tau=\infty$ and find

$$\beta \int_0^\infty (\theta')^2 dt = -V(\theta_u) + V(\theta_\ell). \quad (7)$$

We have used the initial and final conditions $\theta'|_{\tau=0}=0$ and $\theta'|_{\tau=\infty}=0$. Equation (7) gives the energy balance, but unfor-

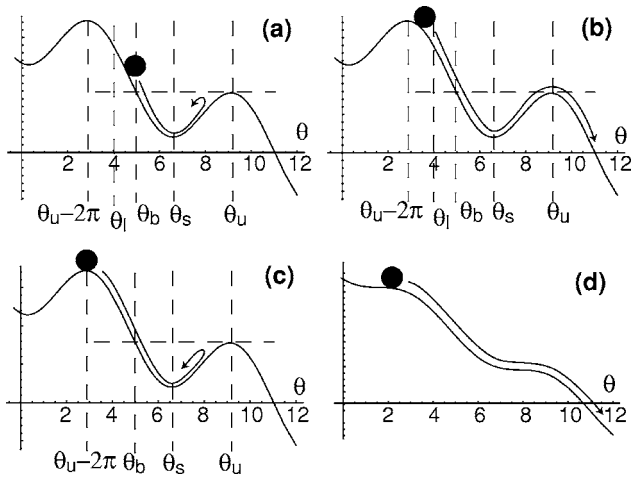


Fig. 5. Motion of a ball in a potential $V(\theta)$ with dissipation. With weak forcing $\gamma=0.3$ and weak damping $\beta < \beta_0$, the ball can either (a) converge to the stable equilibrium or (b) converge to a periodic regime for which loss in energy due to damping is balanced by gain in potential energy, depending on the initial condition. (c) With weak forcing $\gamma=0.3$ and strong damping $\beta > \beta_0$ the only stable state is the stable equilibrium. (d) With strong forcing $\gamma > 1$, the ball falls indefinitely and reaches (asymptotically) a periodic regime.

tunately cannot be solved to find θ_ℓ because we do not know the explicit form of $\theta(\tau)$.

If the pendulum is released with an angle between $\theta_u - 2\pi$ and θ_ℓ , it will reach θ_u with a nonzero velocity and then will continue to rotate. It will accelerate until it reaches (asymptotically) a periodic regime. For this periodic regime $\theta_p(\tau)$, the energy lost by damping during one period must be equal to the gain in potential energy and thus

$$\beta \int_0^T (\theta'_p)^2 d\tau = 2\pi\gamma, \quad (8)$$

where T is the period of the rotations. If we move the pendulum very fast, it will slow down until it reaches (asymptotically) the periodic regime.

For sufficiently large damping, a pendulum started at $\theta_u - 2\pi$ will not reach the next unstable equilibrium, and there are no more oscillations. There is critical damping $\beta_0(\gamma)$ for which $\theta_\ell = \theta_u - 2\pi$. The trajectory that connects two successive unstable points is an homoclinic orbit. The condition of existence of this orbit is given by

$$\beta \int_{-\infty}^{\infty} (\theta'_h)^2 d\tau = 2\pi\gamma, \quad (9)$$

where $\theta_h(\tau)$ represents the homoclinic orbit. The integral is taken between $-\infty$ and $+\infty$ because the trajectory escapes asymptotically from $\theta_u - 2\pi$ and reaches asymptotically θ_u . Below the value $\beta = \beta_0(\gamma)$, the pendulum can rotate and above this value the pendulum will stop at a stable equilibrium. This qualitative change in the behavior is a homoclinic bifurcation, first studied by Andronov.²

B. Hysteresis

When the torque is large ($\gamma > 1$), there is no equilibrium [see Fig. 5(d)]. In the reversible case, the pendulum rotates and accelerates for ever. If there is some dissipation, the

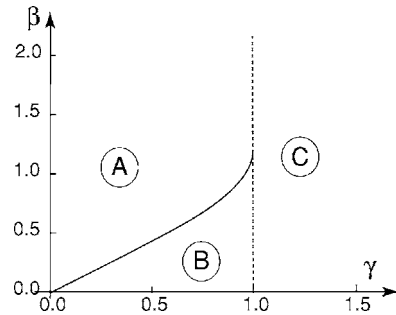


Fig. 6. The two-dimensional parameter space obtained by numerical investigations. Region (a): The only stable solution is the stationary solution; region (b): The stationary solution and the periodic rotation are both stable; region (c): The only stable solution is the periodic rotation.

pendulum will reach a periodic regime. An interesting point is that at the onset of the loss of equilibrium, the behavior can be completely different depending on the damping rate.

If the damping is large (scenario 2), then the periodic regime will be similar to the behavior before the disappearance of equilibrium. The pendulum will slow down when it approaches $\theta = \pi/2$ and stay there a long time, and then it will perform one rotation before returning close to $\theta = \pi/2$. When γ decreases to a value below 1, the pendulum stops at its stable position close to $\pi/2$. There is no hysteresis in this regime.

When the damping is weak (scenario 1), the pendulum starts to rotate and accelerates until it reaches the periodic regime. This regime has a finite period. Actually the pendulum jumps to one periodic trajectory that already existed. When we decrease the forcing torque, even if the critical torque $\gamma = 1$ is crossed, the pendulum keeps on rotating. If we keep on decreasing the torque, the pendulum slows down close to the unstable equilibrium. There is a critical torque for which the pendulum does not cross the unstable equilibrium and returns to the stable one.

C. Summary

There are two boundaries in parameter space (γ, β) (see Fig. 6). One of them is $\gamma = 1$ and corresponds to the disappearance of equilibria. The other one separates the domain where a periodic trajectory exists and the region where it does not exist. The shape of this curve $\beta = \beta_0(\gamma)$ has been obtained by a numerical experiment. There exist three areas in the parameter space that are separated by these boundaries. In region A the only stable solution is the stationary solution. In region B there are two stable solutions, a stationary solution and a periodic rotation. In region C the only stable solution is a periodic rotation.

V. BEHAVIOR NEAR THE BIFURCATIONS

A. Loss of equilibrium

The boundary of the area (in the parameter space) where equilibria exist (regions B and C in Fig. 6) is easily obtained and is given by $\gamma = 1$. For $\gamma > 1$ there is no equilibrium. We are interested in the behavior for $\gamma \approx 1$. In particular, we observed experimentally that for γ slightly above 1 and for high β , the period of oscillations is large and diverges as $\gamma = 1$ is approached. One objective of the following analysis is to characterize this divergence.

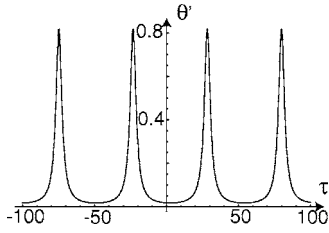


Fig. 7. Plot of the velocity $\theta'(\tau)$ in the high dissipation limit, see Eq. (13), with $\gamma=1.05$ and $\beta=5$.

We first derive an amplitude equation for the behavior of the pendulum close to the loss of equilibrium. We make the ansatz $\gamma=1+\epsilon$ where ϵ is small. In the regime $\epsilon<0$, it is natural to write the angle as $\theta=\pi/2+\theta_1+\dots$. The order of magnitude of the correction of the angle is $\theta_1\sim\sqrt{|\epsilon|}$ because of the parabolic form of the curve $\sin\theta-1$ near $\theta=\pi/2$. We substitute this ansatz in Eq. (2) and obtain to leading order

$$\theta'_1 + \beta\theta'_1 = \epsilon + \frac{1}{2}\theta_1^2. \quad (10)$$

For $\epsilon<0$, the two equilibria are $\theta_1=\pm\sqrt{-2\epsilon}$. Equation (10) gives the time scale of the variation of the angle. If β is not small, the time scale of the variation of θ_1 is given by $\beta\theta'_1\sim\epsilon$, leading to a slow time scale $\sqrt{|\epsilon|}\tau$. The inertial term can then be dropped. Note that for the case $\beta=0$, the time scale is $|\epsilon|^{1/4}\tau$.

This asymptotic analysis offers a description of the system only near the point $\theta=\pi/2$. Thus the periodic orbit for $\gamma>1$ cannot be fully described by this approach. However, when the dissipation is strong enough, that is, when the pendulum does not jump to an existing limit cycle, the pendulum spends a very long time close to the point $\theta=\pi/2$ and the time scale of the period of the rotating motion scales as $|\epsilon|^{-1/2}$.

In the limit of a system dominated by viscosity (β large), it is possible to describe the behavior analytically. If we drop the inertial term θ'' , the equation of motion reduces to

$$\theta' = \frac{1}{\beta}(\gamma - \sin\theta). \quad (11)$$

If we note that for $\gamma>1$,

$$\int \frac{d\theta}{\gamma - \sin\theta} = \frac{2}{\sqrt{\gamma^2 - 1}} \arctan \left[\frac{\gamma \tan(\theta/2) - 1}{\sqrt{\gamma^2 - 1}} \right], \quad (12)$$

we obtain the periodic solution

$$\theta(\tau) = 2 \arctan \left[\sqrt{\frac{\gamma^2 - 1}{\gamma^2}} \tan \left(\frac{\sqrt{\gamma^2 - 1}}{2\beta} \tau \right) + \frac{1}{\gamma} \right]. \quad (13)$$

The origin of time has been set arbitrarily. A plot of the speed of the pendulum as a function of τ (see Fig. 7) reveals that the pendulum spends a long time near $\theta=\pi/2$ (the plateau in the curve). The oscillation period of this solution is

$$T = \frac{2\pi\beta}{\sqrt{\gamma^2 - 1}} \approx \frac{2\pi\beta}{\sqrt{2\epsilon}}, \quad (14)$$

thus confirming that for γ close to 1, the period scales as $\epsilon^{-1/2}$.

B. Loss of rotations

1. Boundary $\beta=\beta_0(\gamma)$

In Fig. 6 we plot the boundary $\beta=\beta_0(\gamma)$ of the region where rotations exist. A point on this curve corresponds to parameters where a homoclinic trajectory connecting two successive unstable points exists. It is, in general, impossible to determine the curve β_0 analytically. However, there is a known situation for which this orbit exists: The pendulum without damping and without forcing. In this case, the first integral corresponding to the energy level of the homoclinic trajectory is

$$\frac{1}{2}(\theta')^2 - \cos\theta = 1. \quad (15)$$

If we slightly perturb the system and add weak forcing and weak damping, we can study the persistence of this solution. We assume that β and γ are both order ϵ . We perturb the solution θ_h and write

$$\theta = \theta_h(\tau) + \epsilon\theta_1(\tau) + \dots \quad (16)$$

In Eq. (2) we use the classical procedure to obtain an energetic balance, that is, we multiply by θ' and integrate between τ_i and τ_f and find

$$\begin{aligned} \frac{1}{2}[(\theta'_f)^2 - (\theta'_i)^2] + \beta \int_{\tau_i}^{\tau_f} (\theta')^2 dt - (\cos\theta_f - \cos\theta_i) \\ = \gamma(\theta_f - \theta_i). \end{aligned} \quad (17)$$

We look for a solution with $\tau_i=-\infty$, $\tau_f=\infty$, $\theta_i=-\pi$, $\theta_f=\pi$, and $\theta'_f=\theta'_i=0$. At order ϵ and in the limit ($\tau_i\rightarrow-\infty$, $\tau_f\rightarrow\infty$), Eq. (17) reads

$$2\pi\gamma = \beta \int_{\tau_i}^{\tau_f} (\theta'_h)^2 ds = \beta \int_{\theta_i}^{\theta_f} \theta'_h d\theta = 8\beta. \quad (18)$$

The integral has been evaluated by using Eq. (15). This equation gives the linear shape of the curve $\beta(\gamma)$ close to the point $\gamma=0$, $\beta=0$.

2. Divergence of the period near the homoclinic bifurcation

When $\beta=\beta_0$, the orbit is $\theta_h(\tau)$. Close to the homoclinic bifurcation, that is, when $\beta\rightarrow\beta_0$, the periodic orbit θ_p has a diverging period. For this orbit, the balance of energy of Eq. (8) can be written as

$$\beta \int_{-T/2}^{T/2} (\theta'_p)^2 d\tau = 2\pi\gamma. \quad (19)$$

The time $T/2$ is defined by $\theta(T/2)=\theta_u$ (unstable equilibrium).

To determine the period of quasi-homoclinic rotations, we use the following reasoning. The left-hand side of Eq. (19) represents the energy lost by viscous damping as the pendulum moves between $\theta_u-2\pi$ and θ_u . Equation (19) tells us that this energy remains constant and is equal to $2\pi\gamma$. Thus, when β decreases slightly, $\beta=\beta_0(1-\epsilon)$, the integral on the left-hand side of Eq. (19) must increase. Moreover for large periods, the pattern between $-T/2$ and $T/2$ is to the first approximation θ_h (Fig. 8). What changes is the period T and in particular, the time spent in the neighborhood of the unstable equilibrium. With these assumptions, the energy bal-

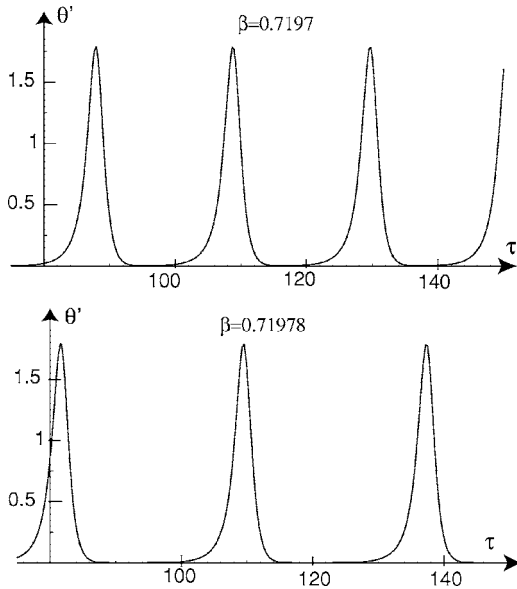


Fig. 8. Plot of the velocity $\theta'(\tau)$ obtained by numerical integration of Eq. (2) close to the homoclinic curve with $\gamma=0.8$ for two values of β . Note that the main difference is the time spent near $\theta'(\tau)=0$.

ance of Eq. (19) offers a way to calculate the variation of the period with β . In Eq. (19) we replace θ_p by θ_h and write

$$\int_{-T/2}^{T/2} (\theta'_h)^2 d\tau = - \int_{-\infty}^{-T/2} (\theta'_h)^2 d\tau + \int_{-\infty}^{\infty} (\theta'_h)^2 d\tau - \int_{T/2}^{\infty} (\theta'_h)^2 d\tau. \quad (20)$$

The second term of the right-hand side is equal to $2\pi\gamma/\beta_0$ [see Eq. (9)]. In Eq. (19), to leading order, we have with $\beta = \beta_0(1 - \epsilon)$

$$\beta_0(1 - \epsilon) \left[- \int_{-\infty}^{-T/2} (\theta'_h)^2 d\tau + \frac{2\pi\gamma}{\beta_0} - \int_{T/2}^{\infty} (\theta'_h)^2 d\tau \right] \approx 2\pi\gamma, \quad (21)$$

or

$$\epsilon 2\pi\gamma \approx -\beta_0 \int_{-\infty}^{-T/2} (\theta'_h)^2 d\tau - \beta_0 \int_{T/2}^{\infty} (\theta'_h)^2 d\tau. \quad (22)$$

To compute the integrals in Eq. (22), we need to characterize the behavior of θ_h near the unstable point. This behavior is dominated by the linear part of Eq. (2). We use the ansatz $\theta = \theta_u + \xi$ and write the linearized equation for ξ as

$$\xi'' + \beta\xi' + (\cos \theta_u)\xi = 0, \quad (23)$$

where $\cos \theta_u = -(1 - \gamma^2)^{1/2}$ is negative. The two characteristic exponents that measure the convergence (divergence) to (from) the unstable point are $a_-(a_+)$ given by

$$a_{\pm} = \frac{\beta}{2} \left(-1 \pm \sqrt{1 - \frac{4 \cos \theta_u}{\beta^2}} \right). \quad (24)$$

We note that $a_- < 0$ and $a_+ > 0$ and $|a_-| > |a_+|$. Thus we have the following scaling

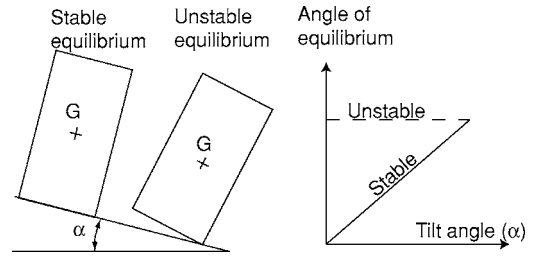


Fig. 9. The equilibrium of a nonsliding solid on an inclined plane. Below a critical tilt angle, there are two equilibria and above it there are no equilibrium. The critical angle depends on the shape of the solid.

$$\theta_h \sim C_- e^{a_+ \tau} \quad \text{as } \tau \rightarrow -\infty, \quad (25a)$$

$$\theta_h \sim C_+ e^{a_- \tau} \quad \text{as } \tau \rightarrow \infty, \quad (25b)$$

where C_- and C_+ are unknown constants.

We can now use these approximations of θ_h to calculate the integrals in Eq. (22). The energy balance is

$$\epsilon 2\pi\gamma \approx -\beta_0 C_-^2 e^{-a_+ T} + \beta_0 C_+^2 e^{a_- T}. \quad (26)$$

As T goes to $+\infty$, the second term of the right-hand side dominates (because $|a_-| > |a_+|$), and thus as ϵ goes to zero, the period of rotation diverges as

$$T \sim \frac{1}{a_-} \log \epsilon. \quad (27)$$

The method used to obtain Eq. (27) can be generalized and the period of a limit cycle approaching an homoclinic bifurcation is generically given by Eq. (27).⁶

VI. SUMMARY AND REMARKS

We have studied both experimentally and theoretically a simple mechanical device: A pendulum forced by a constant torque. The dynamics depends on two parameters: One measures the damping and the other the forcing. The experiment as well as the qualitative analysis reveals the existence of two bifurcations: A local bifurcation, the loss of equilibrium, and a global bifurcation, the homoclinic bifurcation.

For low forcing, the pendulum has two equilibria, one stable and one unstable. For a given forcing ($\gamma=1$), the loss of equilibrium occurs. If the damping is weak, the bifurcation is subcritical and the pendulum rotates with a finite period. If the damping is strong, the bifurcation is supercritical, and the period of rotations just above threshold scales as $1/\sqrt{\epsilon}$, where ϵ is the distance from threshold.

For a given torque and sufficiently weak damping, stable periodic rotations coexist with equilibria. These periodic rotations arise through an homoclinic bifurcation at $\beta = \beta_0(\gamma)$. The exact position of the curve $\beta_0(\gamma)$ in parameter space cannot be determined analytically. The periodic orbit arising through this bifurcation has a period that diverges as $T \sim -\ln \epsilon$.

The qualitative analysis developed here applies to various other physical situations. A typical example is the equilibrium of a nonsliding solid on an inclined plane (Fig. 9). A

model of sandpiles⁷ also exhibits the bifurcations described in our simple experiment. The two bifurcations there correspond to the static angle where the sandpile flows and the dynamical angle (our homoclinic bifurcation), where a finite perturbation leads to avalanches.

^{a)}Professeur à l'Institut Universitaire de France, 103, boulevard Saint-Michel, 75005 Paris, France.

^{b)}Current address: IRPHE, Université de Provence, 49 rue F. Joliot Curie - BP 146. 13384 Marseille cedex 13, France. Electronic address: nvdb@irphe.univ-mrs.fr

¹J. F. Padday and A. R. Pitt, "The stability of axisymmetric menisci," *Philos. Trans. R. Soc. London, Ser. A* **275**, 489–528 (1973).

²A. Andronov, A. Vitt, and S. Khaikin, *Theory of Oscillators* (Pergamon, New York, 1966).

³J. J. Stoker, *Nonlinear Vibrations in Mechanical and Electrical Systems* (Interscience, New York, 1950).

⁴M. Levi, F. C. Hoppensteadt, and W. L. Miranker, "Dynamics of the Josephson junction," *Q. Appl. Math.* **36**, 167–198 (1978).

⁵R. Feynman, R. Leighton, and M. Sands, *The Feynman Lectures on Physics* (Addison-Wesley, Reading, 1963), Vol. 2.

⁶P. Gaspard, "Measurement of the instability rate of a far-from-equilibrium steady state at an infinite period bifurcation," *J. Phys. Chem.* **94**, 1–3 (1990).

⁷L. Quartier, B. Andreotti, S. Douady, and A. Daerr, "Dynamics of a grain on a sandpile model," *Phys. Rev. E* **62**, 8299–8307 (2000).

⁸The kinetic energy of the falling ball is $K=ms^2/2$, where s is the position of the ball in the curvilinear coordinates along the potential.

ONLINE COLOR FIGURES AND AUXILIARY MATERIAL

AJP will now use author-provided color figures for its online version (figures will still be black and white in the print version). Figure captions and references to the figures in the text must be appropriate for both color and black and white versions. There is no extra cost for online color figures.

In addition AJP utilizes the Electronic Physics Auxiliary Publication Service (EPAPS) maintained by the American Institute of Physics (AIP). This low-cost electronic depository contains material supplemental to papers published through AIP. Appropriate materials include digital multimedia (such as audio, movie, computer animations, 3D figures), computer program listings, additional figures, and large tables of data.

More information on both these options can be found at www.kzoo.edu/ajp/.